EXPERIMENTAL STUDIES OF REYNOLDS NUMBER EFFECTS ON SEPARATING, REATTACHING, AND REDEVELOPING FLOW

Simon Song, David B. DeGraaff, John K. Eaton
Department of Mechanical Engineering
Stanford University
Stanford, CA 94305-3030, USA

ABSTRACT

This paper presents an experimental investigation of Reynolds number variation on a separating, reattaching, and redeveloping turbulent boundary layer. This flow is a non-equilibrium boundary layer, meaning that it depends on one or more length scales in addition to the local viscous length scale and boundary layer thickness. These additional scaling dependencies cause the flow to be Reynolds number dependent in some regions. This implies that calculations or experiments based on low Reynolds number data can not be readily scaled up to predict high Reynolds number flows accurately. These experiments were performed using a high Reynolds number flow facility which can achieve momentum thickness Reynolds number up to 30,000 at the inlet of a test section. The mean profile recovers rapidly relative to turbulence statistics downstream of reattachment. The boundary layer separation point depends on Reynolds number, while the reattachment point remains the same at different Reynolds numbers. The flow recovery downstream of reattachment also shows a dependency on Reynolds number in both the mean velocity and turbulence statistics.

INTRODUCTION

Two dimensional flat plate turbulent boundary layers have been explored thoroughly for several decades, and it is generally accepted that the viscous length inner scale and boundary layer thickness outer scale adequately characterize the flow. Most practical engineering flows, however, involve various perturbations which often result in non-equilibrium turbulent boundary layers.

A non-equilibrium turbulent boundary layer can be defined as a boundary layer that has one or more additional length scales beyond the standard inner and outer scales that characterize the flat plate boundary layer. The additional length scales can have different Reynolds number dependencies, which implies that the behavior of the non-equilibrium turbulent boundary layers might change with Reynolds number, and that flow predictions based on low Reynolds number data or models might not be reliable. DeGraaff and Eaton (1999) showed that the turbulent boundary layers over swept and unswept bumps were significantly affected by Reynolds number changes.

Another typical characteristic of non-equilibrium boundary layers is that they recover towards an equilibrium state by developing a *stress equilibrium layer* once the perturbation has been removed. This layer is the region over which the shear stress is in equilibrium with the local wall shear stress. It starts in the inner region, and evolves upward through the boundary layer as the flow proceeds downstream, eventually bringing the entire boundary layer into equilibrium with the wall shear stress. The rate at which the stress equilibrium layer spreads through the boundary layer apparently varies from flow to flow. We believe that it also varies significantly with Reynolds number, although there is not yet a large enough data base to resolve this issue.

The present work addresses a separating, reattaching and redeveloping flow, which develops a typical non-equilibrium boundary layer. A two-dimensional turbulent boundary layer develops on an upstream flat plate, and then flows down a ramp as shown in figure 1. The boundary layer separates on the ramp and reattaches on the downstream flat plate, where it recovers under nearly zero pressure gradient conditions. The mean profile recovers rapidly downstream of the reattachment, but the turbulence statistics recover very slowly. The slow recovery is due to the persistence of large turbulent eddies generated by the Kelvin-Helmholtz

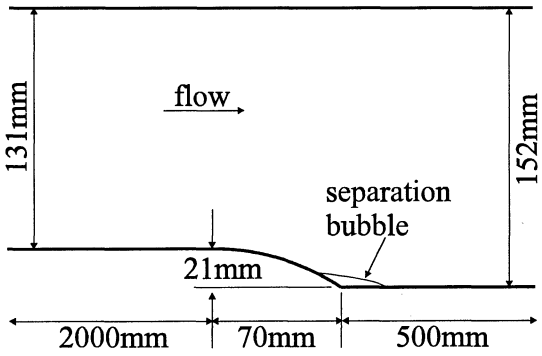

Figure 1. Flow geometry

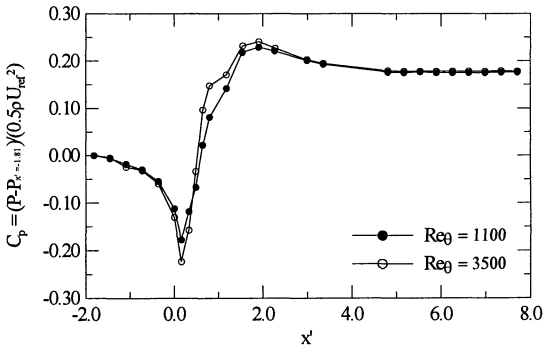

Figure 3. Wall static pressure measurements at the tunnel bottom wall

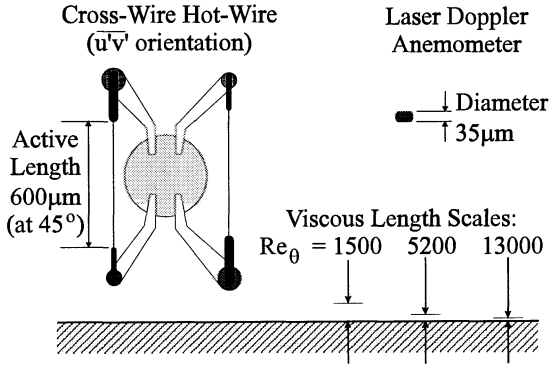

Figure 2. Comparison of LDA and cross-wire hot wire measurement volumes

instability in the separated shear layer (Bradshaw and Wong 1972). In this case, an additional length scale is the height of the inflection point in the mean profile that develops as the flow approaches separation in the adverse pressure gradient. Another possible additional length scale is the thickness of the stress-equilibrium layer which grows out from the wall as the flow recovers to a two dimensional flat plate boundary layer downstream of reattachment. It is important to note that modern CFD codes have are generally not accurate in predicting the recovery downstream of reattachment. This problem is compounded by the Reynolds number dependence of these flows. Most studies of non-equilibrium boundary layers have been done at a single Reynolds number, so there is lack of data that show how these effects vary with Reynolds number.

The objective of this paper is to report the effects of Reynolds number on flow separation and reattachment, and the redevelopment of the turbulent boundary layer downstream of reattachment. The results will provide insight into the complexity of turbulence structure of non-equilibrium boundary layers, and contribute to our understanding of Reynolds number scaling of such flows. So far, two data sets are available: reference station momentum thickness Reynolds numbers, $Re_{\theta,ref}$, of 1100, and 3500. The mean profiles and Reynolds stress profiles will be presented at both Reynolds numbers as well as wall pressure measurements.

FACILITIES AND EXPERIMENTAL TECHNIQUES

The flow geometry is drawn to scale in figure 1. It consists of an upstream flat plate, a smoothly curving ramp, and a downstream flat plate. The ramp is 21 mm in height, *h*, and 70 mm in length. The radius of the ramp curvature is 127 mm. This configuration was designed to produce a small separation bubble based on computations done with NASA's INS2D computer code supplemented with the v^2-f turbulence model developed by Durbin (1993).

The experiments were performed in a moderate scale, closed-loop wind tunnel with a test section cross-section measuring 152 by 711 mm. The wind tunnel is mounted in a large pressure vessel 5.79 m in length by 2.44 m in diameter. By increasing the pressure in the vessel up to 8 atm, and by changing the tunnel speed by factor of 3, a 20:1 momentum thickness Reynolds number range is achieved, while maintaining incompressible flow. Momentum thickness Reynolds numbers up to 30,000 can be achieved at the beginning of the ramp.

The viscous length scale is very small at the highest Reynolds numbers, requiring a high resolution measurement system. We use a custom-built, two-component LDA system with a measurement volume 35 μm in diameter and 60 μm in length as described by DeGraaff and Eaton (1999). Figure 2 shows a scaled drawing which compares the measurement volume size of the LDA system with a conventional cross-wire hot-wire, as well as with the viscous length scales at different Reynolds numbers. The LDA system has more than 1000 times higher spatial resolution than the cross-wire. A Macrodyne frequency domain processor (model 3102) was used to process the Doppler bursts.

Wall static pressure was measured through 0.635 mm diameter surface pressure taps, using a Validyne pressure transducer (model DP 103-10) with the range of 0-0.35 in of H_2O for $Re_{\theta,ref}$ = 1100, and a Setra pressure transducer

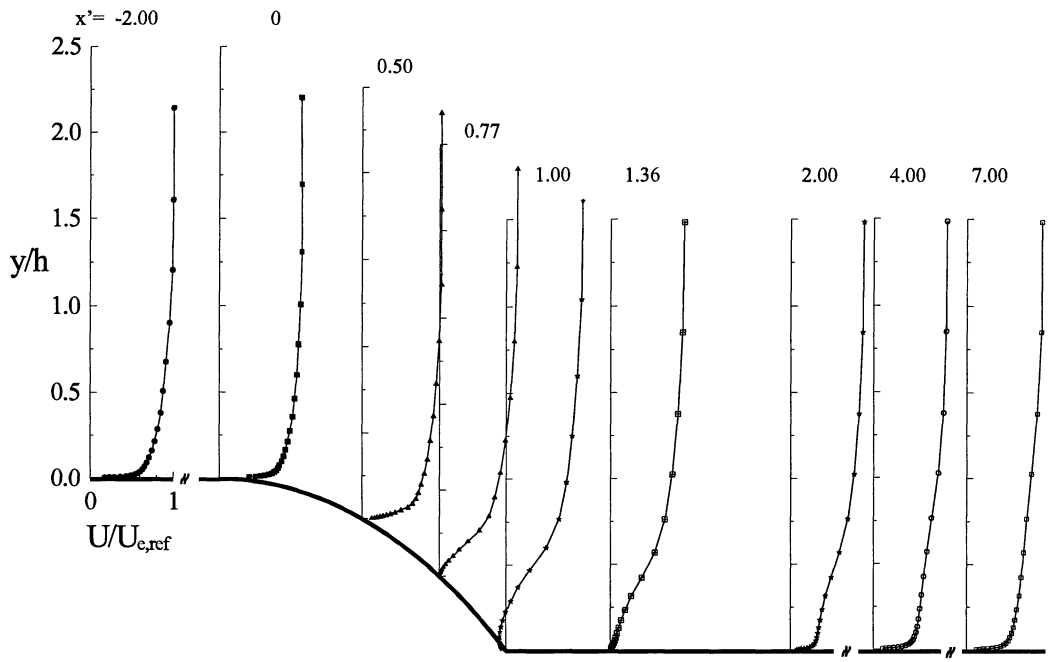

Figure 4. Streamwise mean velocity development for $Re_{\theta,ref}$ = 3500.

(model 264) with the range of 0-25.0 in of H_2O for $Re_{\theta,ref}$ = 3500.

RESULTS AND DISCUSSION

Data are presented in a coordinate system with x in the freestream direction, and y in the wall-normal direction. The y-axis is maintained vertical, and does not follow the curvature of the ramp. A normalized streamwise coordinate, $x'=(x-x_o)/l$, is also used, where x_o corresponds to the beginning of the ramp and l is the ramp length.

All velocity measurements were performed along streamwise stations starting from x' = -2.00 to x' = 7.00. At each streamwise station, the velocity was measured at the center plane of the test section. The reference location is at x' = -2.00 for all velocity measurements, and at x' = -1.81 for wall static pressure measurements.

Figure 3 shows the static pressure coefficient, $C_p = (P-P_{x'=-1.81})/(0.5\rho U_{ref}^2)$, along the tunnel bottom wall for both momentum thickness Reynolds numbers of 1100 and 3500, where ρ is the air density and U_{ref} is the free-stream velocity at the reference station. There is a strong favorable pressure gradient approaching the ramp due to the wall curvature effect before x' = 0.16. After that point, the flow expansion dominates, causing a strong adverse pressure gradient over the rest of the ramp. There is a short plateau in the plot of figure 3 around the trailing edge of the ramp, x' = 1.00, which is most pronounced in $Re_{\theta,ref}$ = 3500 case. This indicates the presence of a separation bubble over the trailing edge. The dividing streamline of the separation bubble acts like a flat wall over a short length around the trailing edge as drawn in figure 1. The adverse pressure gradient region extends to x' = 2.00 although the flow reattaches at x' = 1.36 for both Reynolds numbers. The boundary layer displacement thickness drops rapidly after reattachment, resulting in the mild favorable pressure gradient at x' = 2.00, after which it relaxes back to nearly zero pressure gradient.

The static pressure profiles show significant Reynolds number sensitivity near the ramp trailing edge, where the separation bubble forms. Measured values of C_p are lower for the low Reynolds number case indicating that the separation bubble of $Re_{\theta,ref}$ = 1100 is thicker. The static pressure on the tunnel top wall was also measured for both Reynolds numbers even though the data are not shown here. The data reveal that there is no separation on the top wall, and the plots of C_p for both Reynolds numbers collapse very well.

Figure 4 shows the streamwise mean velocity development for $Re_{\theta,ref}$ = 3500, with the profiles located on the ramp geometry in order to see the streamwise evolution of the flow. The figure is drawn to scale, with the vertical axis expanded twice relative to the horizontal axis in order to see the near wall region more clearly.

The reference mean velocity profile is a typical two-dimensional turbulent boundary layer. As the flow approaches the ramp, the boundary layer gets thinner due to the favorable pressure gradient. The ratio of the boundary layer thickness at the beginning of the ramp to the ramp radius, δ_{99}/R, is 0.175.

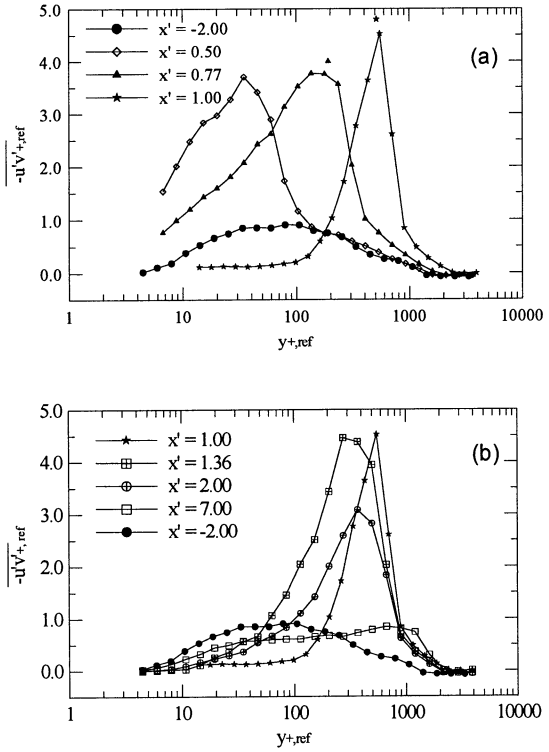

Figure 5. Reynolds shear stress profiles for $Re_{\theta,ref}$ = 3500

Once in the adverse pressure gradient, the mean velocity profiles rapidly develop an inflection point. The boundary layer separates at x' = 0.77 and reattaches at x' = 1.36. The horizontal length of the separation bubble is 41 mm. The back flow in the separation bubble is clearly visible at the trailing edge.

The mean flow recovery is very rapid downstream of reattachment. By x' = 2.00, the profile has filled out considerably, although it still shows a significant deficit in the outer layer. The mean profiles at x' = 4.00 and 7.00, however, have essentially recovered to a flat plate boundary layer.

Figures 5(a) and (b) show the Reynolds shear stress for $Re_{\theta,ref}$ = 3500, normalized with reference inner scaling. The reference profile is a conventional two-dimensional flat plate boundary layer, with a peak value near unity in the lower part of the log region. As the flow passes over the ramp, the shear stress level immediately jumps up even at x' = 0.50 due to the turbulent eddies generated by Kelvin-Helmholtz instability of the separated shear layer. The data are normalized on reference scales, so this increase in Reynolds shear stress is not an artifact of normalizing by the local skin friction. In figure 5(a), the location of the inflection point in the corresponding mean velocity profile is shown by a symbol which is not connected with the other data points.

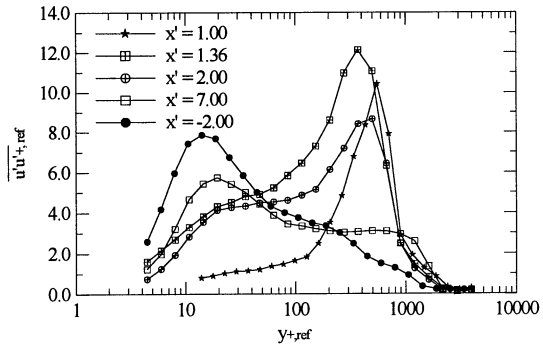

Figure 6. Streamwise Reynolds normal stress profiles for $Re_{\theta,ref}$ = 3500

The energetic eddies appear to be centered at the inflection point, and move away from the wall as the flow separates.

The downstream profiles of Reynolds shear stress are shown in figure 5(b). The reference and the trailing edge profiles are included in figure 5(b) for comparison. The Reynolds shear stress profile recovers very slowly. At x' = 2.00, where the mean profile has largely recovered, the Reynolds shear stress profile is still highly distorted compared with the reference profile. At x' = 7.00, it is clear that the turbulent eddies continue to augment the shear stress in the outer region of the boundary layer. The rise of the shear stress in the inner region, and the decay of the shear stress peaks in the outer region as the flow proceeds downstream indicate the development of the stress equilibrium layer. Given enough distance, the entire boundary layer will recover the equilibrium flat plate shear stress profile. This slow recovery of the turbulence is a typical characteristic of a non-equilibrium boundary layer, and is difficult to predict accurately.

Several streamwise Reynolds normal stress profiles are shown in figure 6 for $Re_{\theta,ref}$ = 3500, again normalized with reference inner scaling. These profiles confirm the slow decay of the turbulence in the recovery region.

To date, there are two complete sets of data for $Re_{\theta,ref}$ = 3500 and 1100. The reference profiles are almost identical for both Reynolds numbers, and the mean and turbulence profiles collapse very well using inner and outer scalings. For both cases, δ_{99} = 25.3mm at the reference station.

In gross features, the $Re_{\theta,ref}$ = 1100 data are similar to the overall flow characteristics for the $Re_{\theta,ref}$ = 3500 case. Both cases show the same growth and decay of the large peak in shear stress centered on the mean velocity inflection point. There are some significant differences in the details, however. Above all, the boundary layer separates at x' = 0.40 for $Re_{\theta,ref}$ = 1100, which is 37% of a ramp length further upstream from the separation point than the $Re_{\theta,ref}$ = 3500 case. This early separation results in the thicker separation bubble as mentioned in the discussion of the wall pressure measurements. Surprisingly, both flows reattach at the same location: x' = 1.36. This initial result

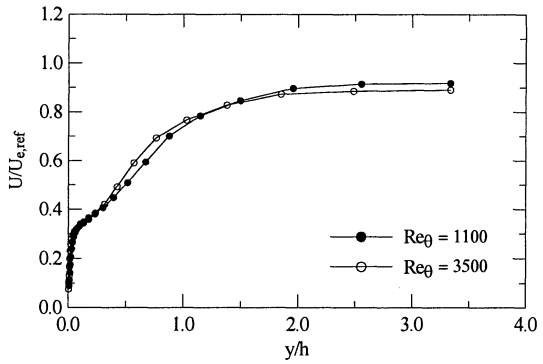

Figure 7. Comparison of mean velocity at x' = 2.00 between $Re_{\theta,ref}$ = 1100 and 3500.

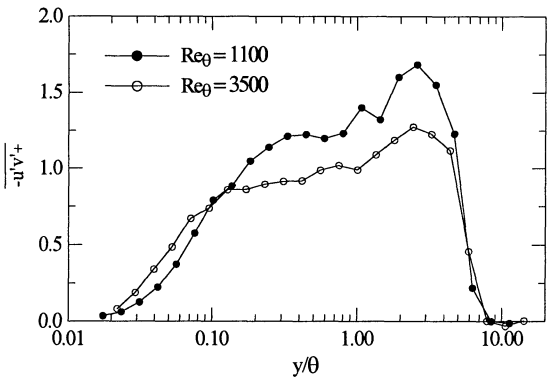

Figure 8. Comparison of Reynolds shear stress at x' = 7.00 between $Re_{\theta,ref}$ = 1100 and 3500.

suggests that the separation point depends on Reynolds number while the reattachment point is mainly affected by the flow geometry, although further investigation is necessary before firm conclusions can be made.

The mean velocity profiles of both Reynolds number at x' = 2.00 are compared in figure 7. The data show that the effects of the flow blockage in the boundary layer are stronger for the lower Reynolds number case, which results in a higher normalized free-stream velocity near y/h = 0.8. This discrepancy also appears the other downstream mean profiles.

Figure 8 shows the Reynolds shear stress for $Re_{\theta,ref}$ = 1100 and 3500 at the most downstream station, x' = 7.00. We have normalized the Reynolds shear stress by the local friction velocity, and the height by the local momentum boundary layer thickness. In these coordinates, the Reynolds shear stress profiles of a two-dimensional flat plate turbulent boundary layer should collapse well. Figure 8 shows a significant discrepancy between the two profiles, however, indicating significant Reynolds number dependency of the recovery rate of the Reynolds shear stress. It is clear that the rate of growth of the stress equilibrium layer is slower for the low Reynolds number case.

CONCLUSION AND FUTURE WORK

We have presented the evolution of the flow down a smoothly curved ramp, and studied the effects of Reynolds number variation on the separation, reattachment, and downstream recovery of the flow. The mean velocity profile recovered very rapidly, while the turbulence statistics had not recovered even by the most downstream measurement location. The separation point was 26 mm further upstream for the low Reynolds number case relative to the high Reynolds number case, while the reattachment point remained the same. The significant Reynolds number effects verify the need for further study of Reynolds number variation on non-equilibrium boundary layers.

Measurements at higher Reynolds numbers are on-going and will allow us to reach firm conclusions about the effects of Reynolds number on non-equilibrium turbulent boundary layers.

ACKNOWLEDGEMENTS

We gratefully acknowledge the financial support of the Office of Naval Research through contract number N 00014-94-0070. Simon Song is supported by a Stanford Graduate Fellowship.

REFERENCES

Bradshaw, P., Wong, F.Y.F., 1972, "The reattachment and relaxation of a turbulent shear layer," *J. Fluid Mech.*, 52, 113-135.

DeGraaff, D. B., and Eaton, J.K., 1999, "Reynolds number scaling of the turbulent boundary layer on a flat plate and on swept and unswept bumps," Technical Report No. TSD-118, Stanford University, Stanford, CA.

Durbin, P., 1993, "Application of a near-wall turbulence model to boundary layers and heat transfer," *International Journal of Heat and Fluid Flow,* 14 No.4, pp. 316-323.